

# Belle II Silicon Vertex Detector (SVD)

1

2 S. Bahinipati<sup>4</sup>, K. Adamczyk<sup>19</sup>, H. Aihara<sup>15</sup>, C. Angelini<sup>8,9</sup>, T. Aziz<sup>7</sup>,  
 3 V. Babu<sup>7</sup>, S. Bacher<sup>19</sup>, E. Barberio<sup>1</sup>, Ti. Baroncelli<sup>1</sup>, To. Baroncelli<sup>1</sup>,  
 4 A. K. Basith<sup>5</sup>, G. Batignani<sup>8,9</sup>, A. Bauer<sup>2</sup>, P. K. Behera<sup>5</sup>, T. Bergauer<sup>2</sup>,  
 5 S. Bettarini<sup>8,9</sup>, B. Bhuyan<sup>6</sup>, T. Bilka<sup>3</sup>, F. Bosi<sup>9</sup>, L. Bosisio<sup>10,11</sup>, A. Bozek<sup>19</sup>,  
 6 F. Buchsteiner<sup>2</sup>, L. Bulla<sup>2</sup>, G. Caria<sup>1</sup>, G. Casarosa<sup>9</sup>, M. Ceccanti<sup>9</sup>,  
 7 D. Červenkov<sup>3</sup>, S. R. Chendvankar<sup>7</sup>, N. Dash<sup>4</sup>, G. De Pietro<sup>8,9</sup>, S. T. Divekar<sup>7</sup>,  
 8 Z. Doležal<sup>3</sup>, D. Dutta<sup>7</sup>, F. Forti<sup>8,9</sup>, M. Friedl<sup>2</sup>, K. Hara<sup>16</sup>, T. Higuchi<sup>12</sup>,  
 9 T. Horiguchi<sup>14</sup>, C. Irmeler<sup>2</sup>, A. Ishikawa<sup>14</sup>, H. B. Jeon<sup>17</sup>, C. Joo<sup>12</sup>, J. Kandra<sup>3</sup>,  
 10 N. Kambara<sup>16</sup>, K. H. Kang<sup>17</sup>, T. Kawasaki<sup>C,13</sup>, P. Kodys<sup>3</sup>, T. Kohriki<sup>16</sup>,  
 11 S. Koike<sup>D,16</sup>, M. M. Kolwalkar<sup>7</sup>, R. Kumar<sup>20</sup>, R. Kumar<sup>15</sup>, P. Kvasnička<sup>3</sup>,  
 12 C. La Licata<sup>10,11</sup>, L. Lanceri<sup>10,11</sup>, J. Lettenbicher<sup>2</sup>, J. Libby<sup>5</sup>, T. Lueck<sup>8,9</sup>,  
 13 M. Maki<sup>16</sup>, P. Mammini<sup>9</sup>, S. N. Mayekar<sup>7</sup>, G. B. Mohanty<sup>7</sup>, S. Mohanty<sup>A,7</sup>,  
 14 T. Morii<sup>12</sup>, K. R. Nakamura<sup>16</sup>, Z. Natkaniec<sup>19</sup>, Y. Onuki<sup>15</sup>, W. Ostrowicz<sup>19</sup>,  
 15 A. Paladino<sup>8,9</sup>, E. Paoloni<sup>8,9</sup>, H. Park<sup>17</sup>, F. Pilo<sup>9</sup>, A. Profeti<sup>9</sup>,  
 16 I. Rashevskaya<sup>B,11</sup>, K. K. Rao<sup>7</sup>, G. Rizzo<sup>8,9</sup>, Resmi P. K<sup>5</sup>, M. Rozanska<sup>19</sup>,  
 17 J. Sasaki<sup>15</sup>, N. Sato<sup>16</sup>, S. Schultschik<sup>2</sup>, C. Schwanda<sup>2</sup>, Y. Seino<sup>13</sup>,  
 18 N. Shimizu<sup>15</sup>, J. Stypula<sup>19</sup>, J. Suzuki<sup>16</sup>, S. Tanaka<sup>16</sup>, G. N. Taylor<sup>1</sup>,  
 19 R. Thalmeier<sup>2</sup>, R. Thomas<sup>7</sup>, T. Tsuboyama<sup>16</sup>, S. Uozumi<sup>17</sup>, P. Urquijo<sup>1</sup>,  
 20 L. Vitale<sup>10,11</sup>, S. Watanuki<sup>14</sup>, M. Watanabe<sup>12</sup>, I. J. Watson<sup>15</sup>, J. Webb<sup>1</sup>,  
 21 J. Wiechczynski<sup>19</sup>, S. Williams<sup>1</sup>, B. Würkner<sup>2</sup>, H. Yamamoto<sup>14</sup>, H. Yin<sup>2</sup>,  
 22 T. Yoshinobu<sup>16</sup>, and L. Zani<sup>8,9</sup>

23

(Belle-II SVD Collaboration)

24 <sup>1</sup> School of Physics, University of Melbourne, Melbourne, Victoria 3010, Australia25 <sup>2</sup> Institute of High Energy Physics, Austrian Academy of Sciences, 1050 Vienna,  
26 Austria27 <sup>3</sup> Faculty of Mathematics and Physics, Charles University, 121 16 Prague, Czech  
28 Republic29 <sup>4</sup> Indian Institute of Technology Bhubaneswar, Satya Nagar, India30 <sup>5</sup> Indian Institute of Technology Madras, Chennai 600036, India31 <sup>6</sup> Indian Institute of Technology Guwahati, Assam 781039, India32 <sup>7</sup> Tata Institute of Fundamental Research, Mumbai 400005, India, <sup>A</sup> also at Utkal  
33 University, Bhubaneswar 751004, India34 <sup>8</sup> Dipartimento di Fisica, Università di Pisa, I-56127 Pisa, Italy35 <sup>9</sup> INFN Sezione di Pisa, I-56127 Pisa, Italy36 <sup>10</sup> Dipartimento di Fisica, Università di Trieste, I-34127 Trieste, Italy37 <sup>11</sup> INFN Sezione di Trieste, I-34127 Trieste, Italy, <sup>B</sup> presently at TIFPA - INFN,  
38 I-38123 Trento, Italy39 <sup>12</sup> Kavli Institute for the Physics and Mathematics of the Universe (WPI),  
40 University of Tokyo, Kashiwa 277-8583, Japan41 <sup>13</sup> Department of Physics, Niigata University, Niigata 950-2181, Japan, <sup>C</sup> presently at  
42 Kitasato University, Sagami-hara 252-0373, Japan43 <sup>14</sup> Department of Physics, Tohoku University, Sendai 980-8578, Japan44 <sup>15</sup> Department of Physics, University of Tokyo, Tokyo 113-0033, Japan

45 <sup>16</sup> High Energy Accelerator Research Organization (KEK), Tsukuba 305-0801,  
46 Japan, <sup>D</sup>deceased  
47 <sup>17</sup> Department of Physics, Kyungpook National University, Daegu 702-701, Korea  
48 <sup>18</sup> H. Niewodniczanski Institute of Nuclear Physics, Krakow 31-342, Poland  
49 <sup>19</sup> Punjab Agricultural University, Ludhiana 141004, India

50 **Abstract.** The Belle II experiment at the SuperKEKB collider in Japan  
51 will operate at an unprecedented luminosity of  $8 \times 10^{35} \text{ cm}^{-2}\text{s}^{-1}$ , about  
52 40 times larger than its predecessor, Belle. Its vertex detector is composed  
53 of a two-layer DEPFET pixel detector (PXD) and a four layer double-  
54 sided silicon microstrip detector (SVD). To achieve a precise decay-vertex  
55 position determination and excellent low-momentum tracking under a  
56 harsh background condition and high trigger rate of 10 kHz, the SVD  
57 employs several innovative techniques. In order to minimize the para-  
58 sitic capacitance in the signal path, 1748 APV25 ASIC chips, which read  
59 out signal from 224k strip channels, are directly mounted on the mod-  
60 ules with the novel Origami concept. The analog signal from APV25  
61 are digitized by a flash ADC system, and sent to the central DAQ as  
62 well as to online tracking system based on SVD hits to provide region  
63 of interests to the PXD for reducing the latter's data size to achieve the  
64 required bandwidth and data storage space. Furthermore, the state-of-  
65 the-art dual phase CO<sub>2</sub> cooling solution has been chosen for a combined  
66 thermal management of the PXD and SVD system. In this proceedings,  
67 we present key design principles, module construction and integration  
68 status of the Belle II SVD.

## 69 1 Introduction

### 70 1.1 SuperKEKB

71 The Belle II experiment [2] is an intensity frontier flavor-factory experiment  
72 that will operate at the SuperKEKB  $e^+e^-$  collider [1] at the KEK laboratory  
73 in Tsukuba, Japan. The primary goals of the experiment are to search for new  
74 sources of CP violation in decays of B and D mesons, which in turn requires  
75 precise determination of decay vertices of B mesons and tagging of D mesons  
76 from the charge of low-momentum pions in  $D^{*\pm} \rightarrow D^0\pi^\pm$ , and to indirectly  
77 look for physics beyond the standard model by studying super-rare decays [3].  
78 The accelerator facility of KEKB will be upgraded to SuperKEKB, that will  
79 run at the same centre-of-mass energy of 10.58 GeV, with a reduced boost of  
80 0.28 as compared to KEKB. In order to achieve the desired physics goals, Belle  
81 II envisions to collect an integrated luminosity of  $50 \text{ ab}^{-1}$ . The design peak  
82 luminosity  $8 \times 10^{35} \text{ cm}^{-2}\text{s}^{-1}$  is 40 times larger than the world record achieved  
83 by Belle. The Belle II detector was successfully "rolled-in" without the vertex  
84 detector happened on April 11, 2017. The commissioning of the main ring of  
85 SuperKEKB started in February 2016.

## 86 1.2 Belle II

87 Belle II detector [4] is a multipurpose instrument, which covers a large solid angle  
88 and has capability for a precise vertex reconstruction and momentum determi-  
89 nation, good pion-kaon separation, and excellent neutral particle identification.  
90 Since high luminosity will warrant high backgrounds and event rates, Belle II  
91 detector has to run under harsh conditions. Therefore, all its sub-detectors need  
92 to be upgraded in order to be able to function at these conditions. The upgraded  
93 detector includes a vertex detector with two pixel and four strip layers, a drift  
94 chamber with long lever arm and small cells, a particle identification system  
95 based on Cherenkov detectors, a fast electromagnetic calorimeter and a muon  
96 detector. Belle II expects to have its first physics run in Fall 2018.

## 97 2 SVD Overview

98 Similar to its predecessor, SuperKEKB will be an asymmetric  $e^+e^-$  collider that  
99 will operate at the  $\Upsilon(4S)$  resonance. This will help in the precise measurement of  
100 CP violation in  $B^0\bar{B}^0$ -pairs, produced close to the interaction point. The two B-  
101 meson decay vertices have to be separable, hence, requiring an excellent impact  
102 parameter resolution. Therefore, in order to cope with high event rate and cater  
103 to the requirement of providing high tracking resolution to reconstruct B-meson  
104 decay vertices, a new vertex detector (VXD) [5] is being built (Figure 1). The  
105 VXD [3] is composed of two systems: a four-layer double-sided strip detector  
106 (SVD) [4] at higher radii around the beam-pipe and a two-layer DEPFET-based  
107 pixel detector (PXD) [5] as the innermost sensing device.

108 In order to minimize multiple scattering and the energy loss of particles  
109 crossing the detectors, the material budget has to be below  $0.2\%X_0$  ( $0.6\%X_0$ )  
110 per layer for the PXD (SVD), including the sensors, readout electronics, support  
111 structures and services. The PXD sensors have pixel pitches ranging from  $50 \times$   
112  $50\mu m^2$  up to  $50 \times 85\mu m^2$  that, together with SVD strip pitches from  $50$ - $75 \mu m$   
113 ( $160$ - $240 \mu m$ ) on the p-side (n-side), results in a combined impact parameter  
114 resolution  $\sigma_{d_0} \approx 15\mu m$ . For low track momenta the impact parameter resolution  
115 is up to three times better than Belle. This improvement decreases for higher  
116 track momenta leading to  $\approx 1.2$  times better  $d_0$  and  $1.7$  times better  $z_0$  impact  
117 parameter resolution [6].

## 118 3 Origami Concept

119 The Belle II SVD is made by four layers of double sided silicon strip detectors  
120 (DSSD) organised in a cylindrical geometry with a polar angle coverage from  
121  $17^\circ$  in the forward region to  $150^\circ$  in the backward region and with a radius going  
122 from  $39$  mm for the inner layer to  $140$  mm for the outer layer.

123 Three different kinds of sensors, fabricated on silicon wafers and with n-type  
124 substrate of  $300 \mu m$  thickness, are used: two rectangular and one trapezoidal.  
125 The latter type is used in the forward region to optimise the angular coverage and

126 the particle incidence angle. The two rectangular sensors are both around 120mm  
 127 long, the larger one being 60 mm wide, the other one 39 mm wide, whereas  
 128 the trapezoidal sensors are around 120 mm long, with the largest (shortest)  
 129 edge around 60 (39) mm wide. The rectangular and trapezoidal sensors are  
 130 made by Hamamatsu Photonics (Japan) and Micron Semiconductor Ltd. (UK),  
 131 respectively. Further details on the sensors can be found in Refs. [7, 8]. Sensors  
 132 are longitudinally organised in ladders, which are made of 2, 3, 4, 5 sensors for  
 133 layer 3 (L3), 4 (L4), 5 (L5), 6 (L6) respectively. From the inner to the outer  
 134 layer 7, 10, 12, 16 ladders will be used to build the barrel shape of every layer.

135 The peripheral sensors in the forward (FW) and backward (BW) region of the  
 136 ladders will be read-out by front end electronics placed on hybrid circuits  
 137 located outside of the SVD active region. It was decided to read-out sensors  
 138 individually, in order to reduce the occupancy of the strips as well as to minimize  
 139 the capacitive load on the front end electronics, keeping the signal-to-noise ratio  
 140 high. This requires the read-out electronics for the inner sensors in layer 4, 5  
 141 and 6 to be placed inside the active area of the SVD, which in turn, led to some  
 142 constraints for the read-out electronics. It must be radiation hard and have a  
 143 short shaping time and low material budget. APV25 [9] fulfils these requirements  
 144 since it is tolerant to radiation doses more than 100 MRad and the combination  
 145 of short shaping time (50 ns) and the online pulse shape processing will keep  
 146 the occupancies below the 1% level even under severe background conditions  
 147 at the SuperKEKB design luminosity. APV25 chips have been thinned from  
 148 the original 300  $\mu\text{m}$  thickness down to 100  $\mu\text{m}$  and placed on top of the sensors  
 149 using the so called "Origami" chip-on-sensor concept [10,11]. Fig. 1 shows various  
 150 components of the SVD in the left and the anatomy of one of the ladders, L6  
 151 with the Origami hybrid in the right.

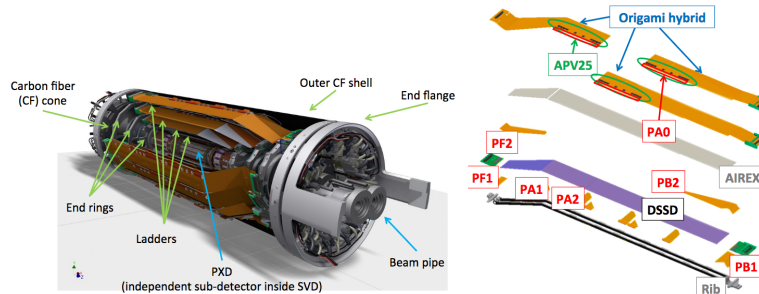


**Fig. 1.** (Left) Components of the Belle II SVD; (Right) Ladder anatomy of an L6 ladder, showing the Origami hybrid, which is a flexible circuit to transmit detector signals to the ladder ends. Here, FlexPA (PA/PF/PB) is flexible circuit to transmit detector signals to the APV25 and PA0 is flexible circuit glued on the Origami hybrid to transmit n-side detector signals to the APV25.

152 The Origami is a three layer kapton hybrid circuit on which all APV25 read-  
153 out chips of one sensor are placed and aligned. The Origami is then glued on  
154 the top side of the sensor, with a 1 mm thick layer of Airex [12] in between,  
155 to ensure electrical and thermal insulation. The sensor top side strips will be  
156 connected to the APV25 chips through a planar flexible pitch adapter circuit,  
157 while the bottom side strips will be routed to the other side of the sensor, toward  
158 the electronics, wrapping two different pitch adapters around the sensor edge,  
159 above the top side wire bondings. Two carbon fiber ribs are used as a support  
160 structure for the ladder.

## 161 4 CO<sub>2</sub> Cooling

162 The alignment of APV25 chips on top of the Origami allows the use of just one  
163 cooling channel, that consists of a 1.6 mm diameter pipe with dual phase CO<sub>2</sub>  
164 flowing inside. This ensure efficient read-out electronics cooling keeping low the  
165 material budget, that is in average 0.6% of a radiation length.

## 166 5 Performance Tests

167 In order to evaluate the performance of sensors, a beam test was performed in  
168 April 2016 at DESY in Germany, using a slice of the VXD that included all  
169 layers. The test was performed with an electron beam of energy 25 GeV and a  
170 solenoid magnetic field up to 1 T.

### 171 5.1 Sensor Performance

172 For the efficiency study, only the four SVD layer data are used to evaluate the  
173 efficiency: once that the layer under study is fixed, the other three layers are used  
174 as a reference, requiring one hit per layer and fitting a track passing through  
175 all 3 reference layers. The fitted track is used to estimate the position of the  
176 hit point on the fourth layer, then the number of hits within 300  $\mu m$  from the  
177 estimated hit point is counted. The sensor efficiency, which is the ratio between  
178 the number of counted hits and the number of fitted tracks, is above 99.5% in  
179 both  $\phi$  and  $z$  directions [13]. The same study was performed on the sensors of  
180 the other layers and the efficiencies show similar results for both strip directions.

### 181 5.2 Sensor Efficiency

182 For calculating resolution, a total of twelve layers that includes four SVD layers,  
183 two PXD layers and six layers of the EUDET telescope, three downstream and  
184 three upstream, are used. This is to avoid a biased estimation of the resolution.  
185 The tracks used to evaluate resolution are required to have at least 10 hits in the  
186 eleven layers used as a reference. The residuals for the sensor under investigation  
187 is calculated as the difference between the position of the extrapolated track and

188 the hit on the sensor, on both  $\phi$  and  $z$  directions [13]. The obtained resolution  
189 estimation is compatible with the digital resolution, which is 7.2(23.1)  $\mu m$  in  
190  $r - \phi(z)$  direction for L3 and 10.8(34.6)  $\mu m$  in  $r - \phi(z)$  direction for L4, L5 and  
191 L6 ladders [13].

### 192 5.3 Ladder Assembly Status

193 Ladder assembly is a complex process [7, 11], that requires precision assembly  
194 jigs ( $O(50\mu m)$ ), on which the sensors are fixed by vacuum chucking followed by  
195 gluing and wire-bonding. The FW and BW subassemblies for L4, L5 and L6  
196 were produced at INFN Pisa, Italy. L3, L4, L5 and L6 production is done at  
197 Melbourne, Australia, TIFR, India, HEPHY, Vienna and Kavli-IPMU, Japan,  
198 respectively. As of May 2017, FW/BW subassembly is almost completed. For  
199 L3, ladder production has finished. For L4, 6 out of 10+2 ladder production is  
200 done. For L5, 12 out of 12+3 ladder production is done and for L6, 7 out of  
201 16+4 ladder production is completed.

### 202 5.4 Mechanical Precision Measurement

203 Mechanical precision are measured with an optical coordinate measuring ma-  
204 chine. A displacement of less than 150  $\mu m$  (nominal value) in all directions for  
205 L4 is obtained. Similar results are obtained for the other three layers.

### 206 5.5 Humidity and Temperature Monitoring

207 During the beam test at DESY, one Dewpoint transmitter and few fibers were  
208 used [14]. The Fiber Optical Sensors (FOS) sensitive to humidity were installed  
209 close to PXD ladders. In the experiment, there will be 4 sniffing pipes, steadily  
210 sampling the dew point with external sensors, two in the cold VXD volume, two  
211 in the warm VXD volume. This work, both for PXD and SVD, will be carried  
212 out at Trieste, Italy. For low humidity/ dew point, these external sensors are  
213 much more precise than the FOS.

### 214 5.6 Background Monitoring

215 Due to the increased luminosity at Belle II, severe beam-induced backgrounds  
216 and integrated radiation doses are expected. The primary background sources  
217 will be Touscheck scattering, radiative Bhabha scattering,  $e^+e^-$  pair production  
218 in photon-photon scattering, and off-momentum particles from beam-gas inter-  
219 actions. Synchrotron-radiation induced backgrounds are expected to be smaller  
220 and can be kept under control by appropriate shielding. These backgrounds  
221 are strongly dependent on beam optics. Simulations show that the most affected  
222 Belle II sub-detector is the VXD with energy losses coming mainly from electrons  
223 and positrons. For the inner layers of the SVD, a dose of about 0.90 kGy/ab<sup>-1</sup>  
224 (90 krad/ab<sup>-1</sup>) would approximately integrate to 45 kGy (4.5 Mrad) [14]. The

225 results from the 15th beam background simulation campaign are consistent with  
226 the results of the last "stable" campaign. The results of the current background  
227 monitoring studies infer that SVD stays within safe limits. New version of SVD  
228 simulation/reconstruction settings for these studies are being prepared (strip  
229 capacitances, noises etc.).

## 230 **6 Summary and Outlook**

231 The Belle II SVD has a partially slanted geometry to reduce material budget  
232 while optimizing the track incidence angle. Novel Origami chip-on-sensor con-  
233 cept has been successfully tested and now in production. Ladder production is  
234 expected to be completed by early 2018. Ladder mount for first half-shell will be  
235 during August 2017. The SVD commissioning is foreseen in October 2018. Belle  
236 II physics run data taking is expected to begin during Fall 2018.

237 *Notes and Comments.* The author thanks all the members of the Belle II SVD  
238 group for their useful comments and suggestions.

## 239 **References**

- 240 1. Y. Ohnishi et al., Prog. Theor. Exp. Phys. (2013) 03A011; see also [http://www-](http://www-superkekb.kek.jp/)  
241 [superkekb.kek.jp/](http://www-superkekb.kek.jp/)
- 242 2. T. Abe et al., Z. Doleal and S.Uno (editors), Belle II Technical Design Report, KEK  
243 Report 2010-1, arXiv:1011.0352; see also <http://belle2.org/>
- 244 3. P. Urquijo, Nuclear and Particle Physics Proceedings, Volumes 263-264, June-July  
245 2015, Pages 15-23.
- 246 4. C. Marinas et al., PoS DIS2016 (2016) 261.
- 247 5. G. Casarosa, PoS EPS -HEP2015 (2015) 255.
- 248 6. A. Paladino et al., PoS ICHEP2016 (2016) 248.
- 249 7. T. Bergauer, PoS (EPS-HEP 2013) 487.
- 250 8. T. Bergauer et al., Nucl. Instr. Meth. A 718 (2013) 279-282.
- 251 9. M. French et al., Nucl. Instr. Meth. A 466 (2001) 359-365.
- 252 10. M. Friedl et al., TWEPP-08, CERN-2008-008 (2008), 277-281.
- 253 11. C. Irmler, TWEPP-12, 2013 JINST 8 (TWEPP 2012 conference), C01014.
- 254 12. Airex AG (Switzerland), <http://www.airexag.ch>.
- 255 13. T. Luck et al., PoS Vertex2016 (2016) 057.
- 256 14. L. Vitale et al., PoS Vertex2016 (2016) 051.